MODELLING SHEAR MECHANISMS IN FRP-STRENGTHENED R/C BEAMS

Marco MENEGOTTO[a], Giorgio MONTI[b], Marc'Antonio LIOTTA[c]

[a] Prof.; Sapienza, University of Rome - via A. Gramsci 53, Rome, Italy
E-mail address: *marco.menegotto@uniroma1.it*

[b] Prof.; Sapienza, University of Rome - via A. Gramsci 53, Rome, Italy

[c] Dr.; Sapienza, University of Rome - via A. Gramsci 53, Rome, Italy

Received: 08.05.2009; Revised: 12.05.09; Accepted: 15.06.09

A b s t r a c t

In order to obtain a clear understanding of the mechanisms underlying the shear strengthening of concrete beams by fibre reinforced polymers (FRP), an extended experimental work was performed and analytical model has been developed to reproduce rationally the tests' features.
In the model, through the definition of (i) the generalised constitutive law of a FRP sheet bonded to concrete, (ii) the compatibility required by the shear crack opening, and (iii) appropriate boundary conditions, depending on the strengthening pattern, the analytical relationships of the stress field in a FRP sheet crossing a shear crack are obtained.
These permit to define closed-form equations for the resistance of shear strengthening by FRP strips or sheets, as function of adopted strengthening pattern and of some basic geometric and mechanical parameters. Contribution of the FRP strengthening is then added to those of concrete and reinforcing steel, adequately weighed.
The model's accuracy has been verified through correlation studies with experimental results, obtained from the literature and from laboratory tests on purposely under-designed real-scale beam specimens, strengthened with different FRP schemes.

S t r e s z c z e n i e

W celu uzyskania pełnego zrozumienia mechanizmów będących podstawą wzmacniania na ścinanie belek za pomocą polimerów zbrojonych włóknami (FRP) podjęto szerokie prace doświadczalne i rozwinięto modele analityczne, aby racjonalnie ująć obserwacje z badań.
Na podstawie określenia: (i) uogólnionych praw konstytutywnych dla elementów FRP połączonych przez przyczepność z betonem, (ii) zgodności wymaganej przy wystąpieniu rys od ścinania, i (iii) odpowiednich warunków brzegowych – uzyskano w modelu analityczne zależności, zależnie od układu wzmocnienia, dla rozkładu naprężeń w elemencie FRP przecinającego rysę. To pozwoliło na określenie ścisłej formy równań w odniesieniu do nośności wzmocnienia za pomocą taśm lub mat FRP jako funkcji zastosowanego układu wzmocnienia oraz niektórych podstawowych paramentów geometrycznych i mechanicznych. Udział wzmocnienia z FRP jest wtedy dodawany z odpowiednią wagą do nośności betonu i zbrojenia na ścinanie.
Poprawność modelu została zweryfikowana przez porównanie zgodności z wynikami eksperymentalnymi uzyskanymi z literatury oraz z własnych badań laboratoryjnych na elementach w skali naturalnej zaprojektowanych do tego celu i wzmocnionych w różny sposób za pomocą FRP.

K e y w o r d s: **Analytical models; Experimental tests; Fibre reinforced polymers (FRP); Shear-resistant mechanisms; Strengthening; Structural concrete.**

1. INTRODUCTION

From current literature and code review, a lack emerges in the mechanisms governing shear strengthening of reinforced concrete members by FRP: the development of practical and reliable design equations is still hindered by three aspects, yet not perfectly understood.

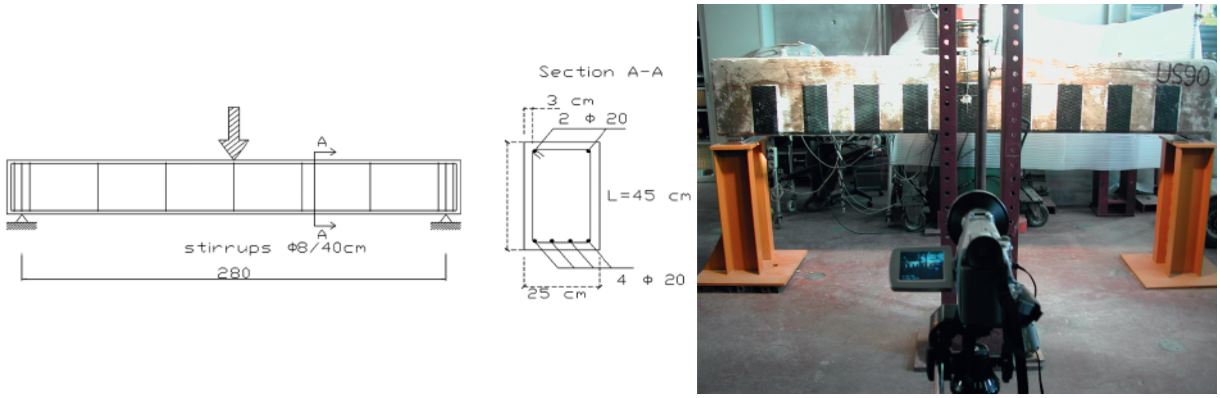

Figure 1.
Specimen dimensions and loading scheme (left), and view (right)

The first aspect regards mechanism that develops when FRP strips/sheets are side bonded to concrete elements: in this case, a "crack-bridging" mechanism activates, similar to the aggregate interlock, dowel effect and concrete tooth; whereas, when the FRP strips/sheets are U-jacketed or fully wrapped around the element, a kind Mörsch truss resisting mechanism is mobilised.

The second aspect regards correct evaluation of transverse stress distribution within an FRP sheet: in fact, a *variable* tensile stress develops in it across the crack profile. This can be conveniently expressed through an *effective* stress, whose intensity is usually given in literature by means of graphs rather than of closed-form equations.

The third aspect regards evaluation of the relative contributions of concrete, steel and FRP to the ultimate shear capacity: it is not guaranteed that both concrete struts and steel stirrups can exploit their full strength, in presence of FRP strengthening.

The objective of this paper is to clarify these aspects, treating them analytically and validating them by means of experimental evidence.

2. EXPERIMENTAL TESTS

2.1. Specimens' geometry and materials

Twenty-nine beam specimens, purposely designed as under-reinforced in shear, were tested with a 3-point loading scheme, all having the same materials and geometry. Some were already presented in [1], [15] and [30].

The beams dimensions were: span 2.80 m, cross-section: 250 mm x 450 mm; longitudinal reinforcement: 4ϕ20 mm bottom and 2ϕ20 top; transverse reinforcement: stirrups ϕ8@400 mm. In view of externally bonding FRP strips, the beams corners were rounded with 30 mm radius. Materials properties were chosen to represent old construction standards: concrete mean compressive cubic strength: R_{cm} = 13.3 MPa; steel rebars mean yield strength: f_{ym} = 500 MPa. All external strengthening was done with a single layer of CFRP strips/sheet 0.22 mm thick and with elastic modulus E_f = 390 GPa.

Figure 1 shows specimen's dimensions and loading scheme. The FRP strengthening strips, when not fully wrapped, end at 150 mm from the beam top, to simulate application in presence of a slab. Terminology is illustrated in Table 1.

2.2. Description and results

All tests are described, pointing out their load and mode of failure.

Strips spacing is measured along the beam axis. Side bonding, U-jacketing and Wrapping around the cross-section are referred to as S-, U-, and W-strengthening, respectively. Note that S-strengthening is only considered for non-seismic applications. The first letter denotes the cross-section strengthening scheme (S, U or W), the second letter denotes discrete strips (S) or continuous fabric (F), the number denotes the angle of the fibres. An additional '+' denotes the presence of a collaboration strip on the beam side along the bottom corner. The notation used to identify each test, according to the strengthening scheme, is represented in Table 1.

Reported cracks are those due to shear, while flexural cracks were regularly observed at around 90-100 kN load. Failure was always due to shear.

Several different patterns were designed. Their shear capacity has been determined analytically, then and the actual specimens have been tested. Two subse-

Table 1.
Strengthening scheme, notation and experimental shear capacity of the tested beams

STRENGTHENING APPLICATION	STRENGTHEN-ING TYPE	FIBRES ANGLE	NAME	STRENGTHENING PATTERN	SHEAR CAPACITY (kN)
NONE/AS BUILT	NONE	-	REF 1 to 4	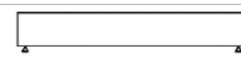	98.0 (average)
SIDE BONDING	STRIPS width 150 mm spacing 300 mm	90°	SS90*	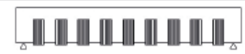	100.0
		45°	SS45*		101.0
		60°, 45°, 30°	SSVA		105.0
	SHEETS	90°	SF90		112.5
U-JACKETING	STRIPS width 150 mm spacing 300 mm	90°	US90*	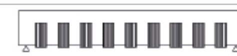	95.0
		60°	US60		111.0
		60°, 45°, 30°	USVA		120.0
		60°, 45°, 30°	USVA+		135.0
		45°	US45+		126.0
		45°	US45		155.0
		90°	US90(2)*	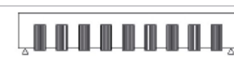	90.0
		90°	US90+	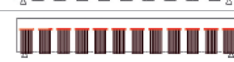	133.0
	STRIPS width 150 mm spacing 300 mm	45°	US45+ "D"		164.5
		45°	US45++"E"	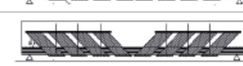	163.5
		45°	US45++"F"		150.0
	STRIPS width 50 mm spacing 100 mm	45°	US45++		133.5
	SHEETS	45°	UF45+ "A"	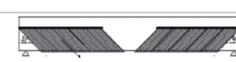	167.0
		45°	UF45++"B"		172.0
		45°	UF45++"C"		183.0
		45°	UF45	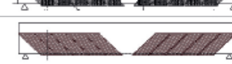	168.0
		90°	UF90		125.0
		90°	UF90+		163.0
WRAPPING	STRIPS width 150 mm spacing 300 mm	45°	WS45	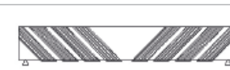	177.3
	STRIPS width 50 mm spacing 100 mm	45°	WS45+		158.5
	SHEETS	45°	WF45	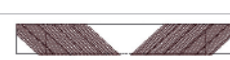	186.1

* In these tests, shear cracks did not fully activate the FRP strips, which then did not contribute to the shear strength

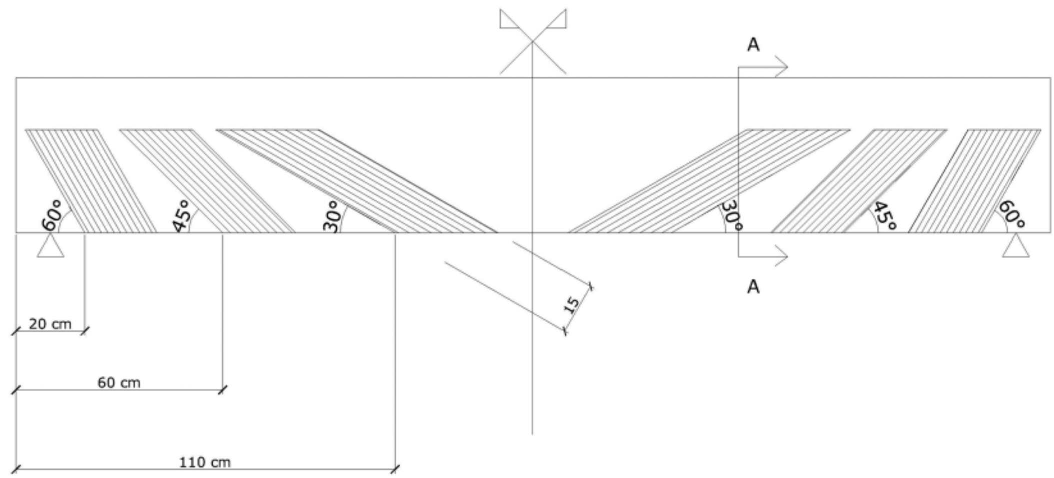

Figure 2.
Configuration of SSVA strengthening

quent test series have been performed, in order to correct problems possibly arising during the first one.

Two concrete cube specimens were tested at the start of each series, in order to check constancy of properties.

Strengthening was performed with vertical (90°) and 45°-inclined FRP strips or fabrics. Variable inclination patterns were tested (SSVA, USVA, USVA+ specimens), too (Fig. 2).

The first series of tests led to an interesting remark, related to the strips spacing, which should be sufficiently narrow, to ensure cracks crossing at least one strip. If strips are too widely spaced, shear cracks can actually develop without crossing them in the effectively bonded region. In this case, especially in case of Side-bonding, a field exists where a crack passes in between strips without crossing and activating them. This field is defined by possible minimum and maximum slope of the crack (Fig. 3). From the same figure, it can be seen that the extension of such field reduces when passing from S- to U-strengthening and also by increasing the fibre inclination.

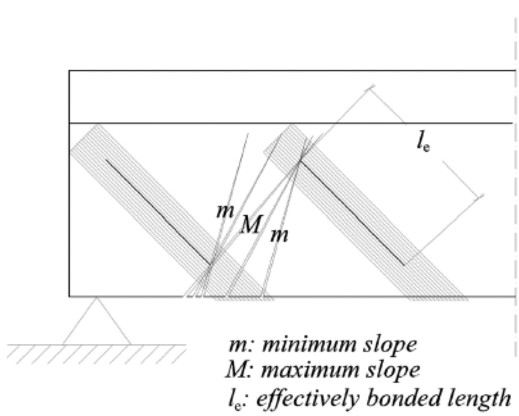

Figure 3.
Field, defined by the minimum (m) and maximum (M) possible crack slope, where cracks can form without crossing the strips, due to excessive strip spacing. Cracks forming outside such field do activate the strips

Observation of tested specimens and the comparison with theoretical results, shown in section 4, suggest that the width w_f and the spacing p_f of the strips, measured orthogonally to the angle β of the direction of the fibres crossing the cracks, should be:

$50 \text{ mm} \leq w_f \leq 250 \text{ mm}$;

$2\, w_f \leq p_f \leq \min\{0.5\, d,\ 3\, w_f,\ w_f + 200 \text{ mm}\}$

The second series of tests was then carried out, complying with the above limitations. In the tests denoted with '+', the top ends of the U-jacketed strips were mechanically anchored through FRP rebars. In those denoted with '++', in addition to the top mechanical anchorage, a collaboration strip along the beam bottom corner was applied.

3. DESIGN EQUATIONS FOR FRP SHEAR STRENGTHENING

In this section, a consistent analytical framework for describing behaviour of RC elements FRP-strengthened in shear is presented, following previous efforts made by several authors ([2], [3], [4], [5], [6], [7]). The theory described below has already been presented in detail in [30].

Developed theory arrives at the description of the FRP stress distribution $\sigma_{f,cr}(x)$ along a shear crack (as

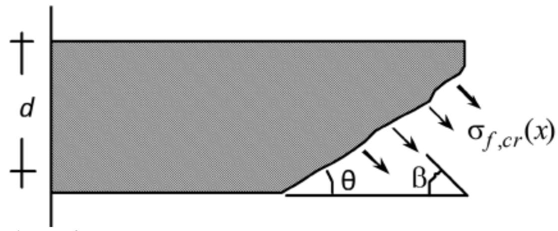

Figure 4.
Stress distribution along an FRP sheet crossing a shear crack

qualitatively sketched in Figure 4), through closed-form equations, as opposed to existing regression-based formulas (e.g., [8], [9]).

Once $\sigma_{f,cr}(x)$ is correctly defined, the FRP resultant force across the crack is computed and the FRP contribution to the shear capacity is found. The analytical developments yield three predictive equations, for Side Bonding (S), U-jacketing (U) and Wrapping (W), respectively.

The equations are given in terms of the available geometrical and mechanical parameters of FRP strengthening and RC beam and compute the FRP shear contribution, to be added to those of concrete and transverse reinforcement for finding the overall shear capacity. These equations have been incorporated into the Code for FRP strengthening recently issued by the Italian Research Council (CNR) [10], illustrated also at AMCM 2005 Conference [11]. In the following, the formulae relevant to the FRP debonding are those of that Code.

The assumptions are (Figure 5):

- Shear cracks are evenly spaced along the beam axis, and inclined at an angle θ,
- At ULS, the cracks depth is equal to the internal lever arm $z = 0.9\, d$,
- In case of U-jacketing (U) and wrapping (W), the resisting mechanism is based on Mörsch truss, while in case of side bonding (S), the mechanism of "crack-bridging" is considered, as the tensile diagonal tie is missing and a Mörsch truss cannot form.

In order to fully characterize the physical phenomenon, the following aspects must be analytically defined: i) failure criterion of an FRP strip/sheet bonded to concrete; ii) generalised stress-slip constitutive law; iii) compatibility equations (i.e., the crack opening); iiii) boundary conditions (i.e., the available bonded length on both sides of the crack, depending on the strengthening pattern).

3.1. Generalised failure criterion of an FRP strip/sheet bonded to concrete

The criterion should include both possible cases:

a) straight strip/sheet

b) strip/sheet wrapped around a corner.

For case a), two parameters are introduced: the *effective bond length* l_e (also referred to as *optimal anchorage length*) and the *debonding strength* f_{fdd}. For both, several different equations have been proposed (e.g., [12], [13]). In this paper, as said above, the equations of the Code [10] are used.

The effective bond length can be given as [10]:

$$l_e = \sqrt{E_f t_f / 2 f_{ctm}} \qquad \text{[length in mm]} \qquad (1)$$

where: E_f = FRP sheet elastic modulus, t_f = sheet thickness, $f_{ctm} = 0.27 \cdot R_{ck}^{2/3}$ = concrete mean tensile strength (with R_{ck} = concrete characteristic cubic strength).

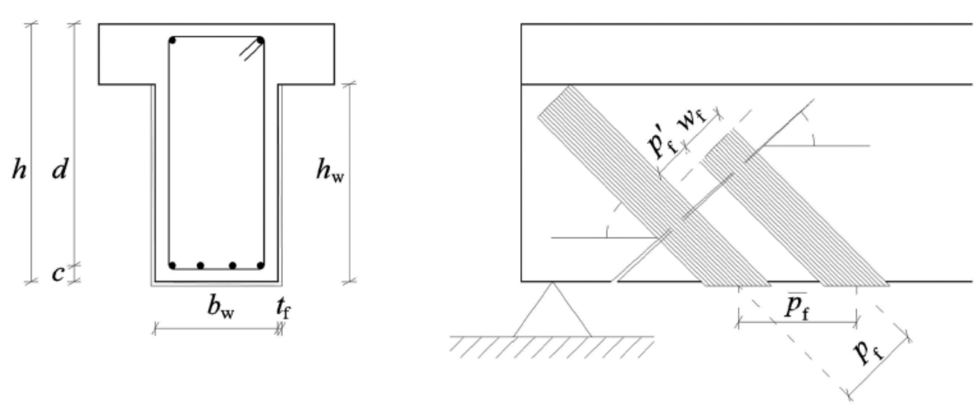

Figure 5.
Geometry notation

The debonding strength can be given as [10]:

$$f_{fdd} = 0.80/\gamma_{f,d}\sqrt{2\,E_f\,\Gamma_{Fk}/t_f} \quad \text{units: [N, mm]} \qquad (2)$$

where $\gamma_{f,d}$ is a partial safety factor, depending on application quality, and Γ_{Fk} is a specific fracture energy of the FRP-concrete bond interface, expressed as [10]:

$$\Gamma_{Fk} = 0.03 \cdot k_b \cdot \sqrt{f_{ck} \cdot f_{ctm}} \quad \text{units: [N, mm]} \qquad (3)$$

$k_b = 1$ for sheets; for strips, covering/scale coefficient, is given as:

$$k_b = \sqrt{\left(2 - w_f/p_f\right)/\left(1 + w_f/400\right)} \geq 1 \qquad (4)$$

with: w_f = width measured orthogonally to β; p_f = spacing in same direction;

However, w_f should not exceed min $(0.9d, h_w)\cdot\sin(\theta+\beta)/\sin\theta$

with d = beam effective depth, h_w = beam web depth, β = angle of strip/sheet to the beam axis, θ = crack angle to the beam axis.

In case the available bond length l_b is lower than the effective bond length l_e, the debonding strength is reduced accordingly:

$$f_{fdd}(l_b) = f_{fdd} \cdot l_b/l_e\left(2 - l_b/l_e\right) \quad (\text{if } l_b < l_e) \qquad (5)$$

For case b) (wrapped around a corner) the FRP strip attains a fraction ϕ_R of its ultimate strength f_{fu} depending on the ratio of rounding radius r_c to the beam width b_w [14]:

$$\phi_R = 0.2 + 1.6\; r_c/b_w, \qquad 0 \leq r_c/b_w \leq 0.5 \qquad (6)$$

Thus, including both cases a) and b), the ultimate strength of the FRP strip/sheet is:

$$f_{fu}(l_b, \delta_e, r_c) = f_{fdd}(l_b) + \left\langle \phi_R \cdot f_{fu} - f_{fdd}(l_b) \right\rangle \cdot \delta_e \qquad (7)$$

where: $\delta_e = \begin{cases} 0 & \text{free end} \\ 1 & \text{end around a corner} \end{cases}$

and where $\langle . \rangle$ denotes that the bracketed expression is zero if negative.

If $l_b \geq l_e$, the ultimate strength of the FRP strip/sheet, wrapped around a corner is simply:

$$f_{fu}(r_c) = f_{fdd} + \left\langle \phi_R \cdot f_{fu} - f_{fdd} \right\rangle \qquad (8)$$

3.2. Generalised stress-slip constitutive law

The generalised stress-slip law of FRP strips/sheets bonded to concrete, including both cases of free end or wrapped around a corner, is given as (symbols in Figure 6):

$$\sigma_f(u, l_b, \delta_e) = \begin{cases} f_{fdd} \cdot \sin(\pi/2 \cdot u/u_1) & \text{if} \quad u < u_1(l_b) \\ f_{fdd} & \text{if} \quad u_1(l\ ) \leq u < u_d(l_b) \\ f_{fdd} \cdot \left(\cos\left((u - u_d)/u_1 \cdot \pi/2 \cdot (1 - \delta_e)\right)\right) & \text{if} \quad u_d(l_b) \leq u < u_u(l_b, \delta_e) \\ f_{fdd} \cdot \delta_e + E_f/l_b \cdot (u - u_u) & \text{if} \quad u_u(l_b, \delta_e) \leq u < u_f(l_b, \delta_e, r_c) \\ 0 & \text{if} \quad u_f(l_b, \delta_e, r_c) \leq u \end{cases} \qquad (9)$$

Phase 1 in Figure 6: $u_1(l_b) = \min\{u_1\, l_b/l_e\, ,\, u_1\}$ is the slip at the onset of debonding at the pulled end, as function of the available bond length l_b (up to either the free end or the corner rounding), where u_1 is [29]:

$$u_1 = 1.1 \cdot k_b \cdot c_4 \quad \text{with } c_4 = 0.3\,mm \qquad (10)$$

Phase 2 in Figure 6: $u_d(l_b) = u_1(l_b) + \varepsilon_{fdd} \cdot \langle l_b - l_e \rangle$ is the pulled end slip at complete debonding over the length $l_b - l_e$, where $\varepsilon_{fdd} = f_{fdd} / E_f$ = strain in the straight portion up to the corner rounding and where $\langle . \rangle$ means the content is zero if negative.

Phase 3 in Figure 6: $u_u(l_b) = u_d(l_b) + u_1(l_b)$ = slip at complete debonding of the strip/sheet over the entire length l_b (the strip/sheet can go beyond this slip only if wrapped around a corner).

Phase 4 in Figure 7: when total debonding has occurred, the strip/sheet behaves as a pulled truss of stiffness l_b/E_f up to the ultimate strength, attained at the slip: $u_f(l_b, \delta_e, r_c) = u_u(l_b) + \langle f_{fu}(l_b, \delta_e, r_c) - f_{fdd}(l_b) \rangle \cdot l_b/E_f$; note that $u_f(l_b, \delta_e, r_c) = u_u(l_b)$, for strip/sheet with free end (with $\delta_e = 0$, and therefore with $f_{fu}(l_b, \delta_e, R) = f_{fdd}(l_b)$).

The generalised stress-slip constitutive law also includes particular (and rare) case of free end with $l_b < l_e$ (Figure 6, bottom).

3.3. Compatibility (crack width)

Considering a reference system with the origin at the tip of the shear crack and abscissa x along the crack itself (Figure 8, top left), the crack width (normal to the crack axis) is expressed as $w = w(x)$ In order to obtain closed-form equations, a linear expression is chosen:

$$w(x) = \alpha \cdot x \qquad (11)$$

where α is the crack opening angle.

Phase 1
(sufficient bond length)

Phase 2
(sufficient bond length)

Phase 3
(sufficient bond length)

Phase 1
(insufficient bond length)

Phase 2 and 3
(insufficient bond length)

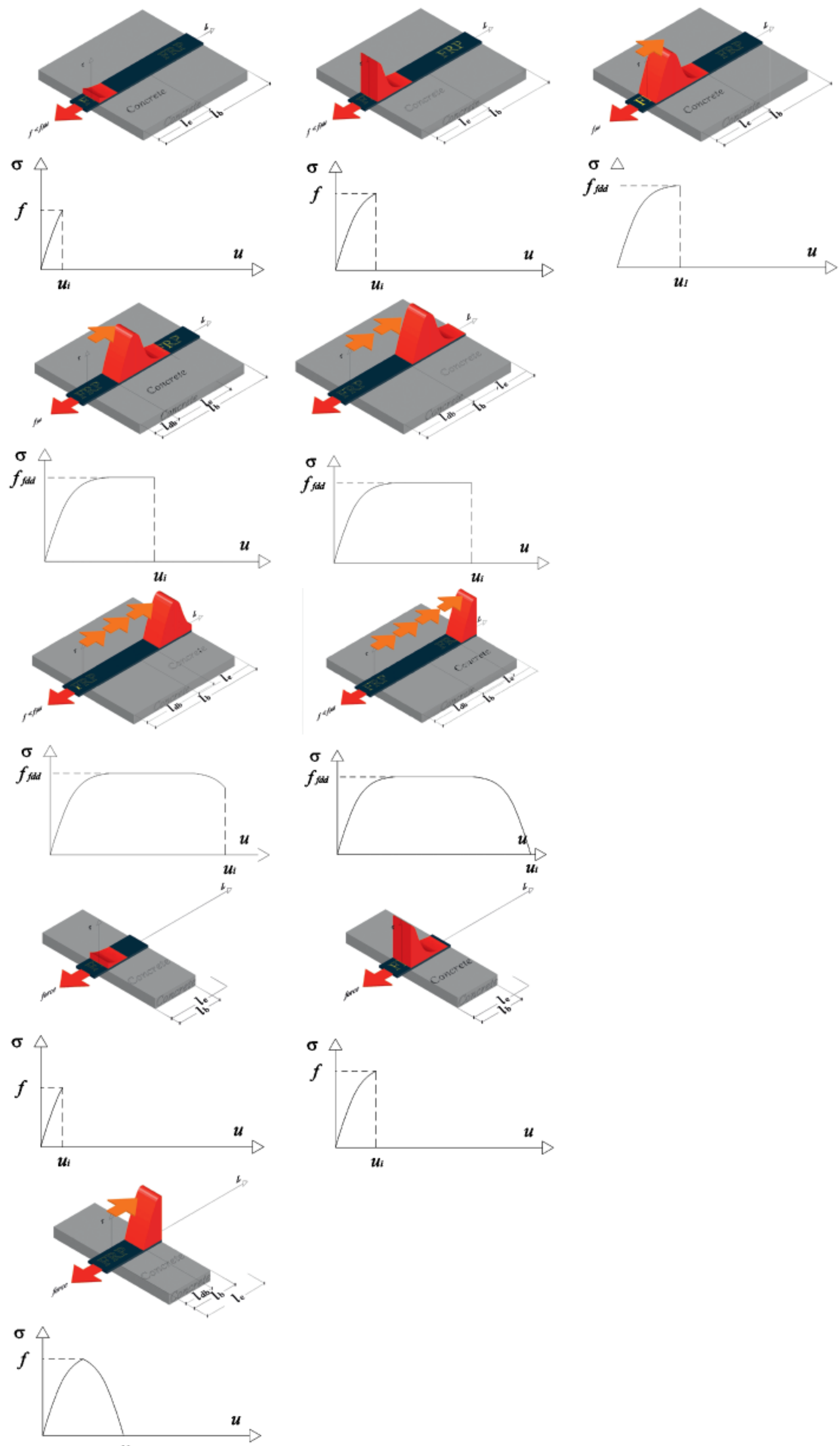

Figure 6.
Stress-slip law for the case of FRP strip/sheet with free end. With sufficient bond length (top 7 figures), and with small bond length (bottom 3 figures). The stress-slip σ_f-u diagrams correspond to the different positions of the bond stress field σ_f (l_b) along the bonded length

Phase 4
(sufficient bond length)

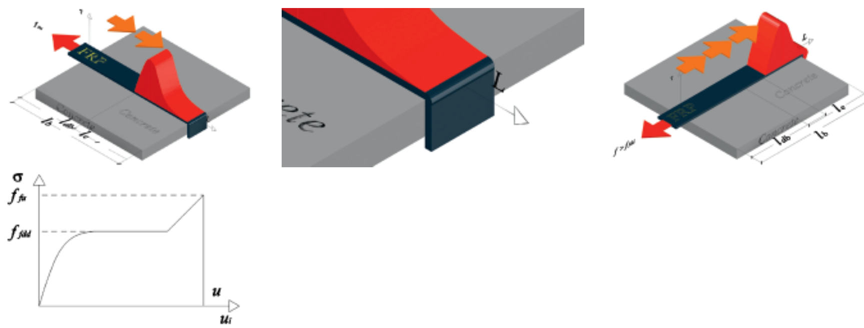

Figure 7.
Stress vs. slip for FRP strip/sheet wrapped around a corner. Numbers on the stress-slip σ_f -u diagram correspond to different positions of the bond stress field σ_f (l_b) along the bonded length

For symmetry at crack edges, the slip, imposed to the strip/sheet crossing it, is:

$$u(\alpha, x) = w(x)/2 \cdot \sin(\theta+\beta) = \alpha/2 \cdot x \cdot \sin(\theta+\beta) \quad (12)$$

3.4. Boundary conditions (available bond length)

The boundary conditions refer to the available bond length $l_b(x)$ on both sides of the shear crack and should be defined according to the strengthening scheme adopted: either S, U, W. Figure 8 depicts the following definitions:

$$l_b(x) = \begin{cases} \min\{\, l_{b,top}(x), l_{b,bot}(x) \,\} & \text{S = Side bonding} \\ l_{b,top}(x) & \text{U = U-jacketing} \\ \max\{\, l_{b,top}(x), l_{b,bot}(x) \,\} & \text{W = Wrapping} \end{cases} \quad (13)$$

where: $l_{b,top}(x)$, $l_{b,bot}(x)$ are the available bond lengths, starting from the crack axis, towards the strip/sheet top and bottom end, respectively.
More analytical details can be found in [15].

3.5. FRP stress profile along the shear crack

In order to obtain the FRP stress profile along the crack $\delta_{f,cr}(x)$, including compatibility (crack opening) and boundary (available bond length) conditions, one has to substitute into the constitutive law δ_f (u, l_b, δ_e):

- the compatibility equation $u = u(\alpha, x)$ given by (12),
- the boundary condition $l_b = l_b(x)$ given by (13), and

c) the appropriate value of δ_e depending on the end constraint (= 0 for S and U; = 1 for W).

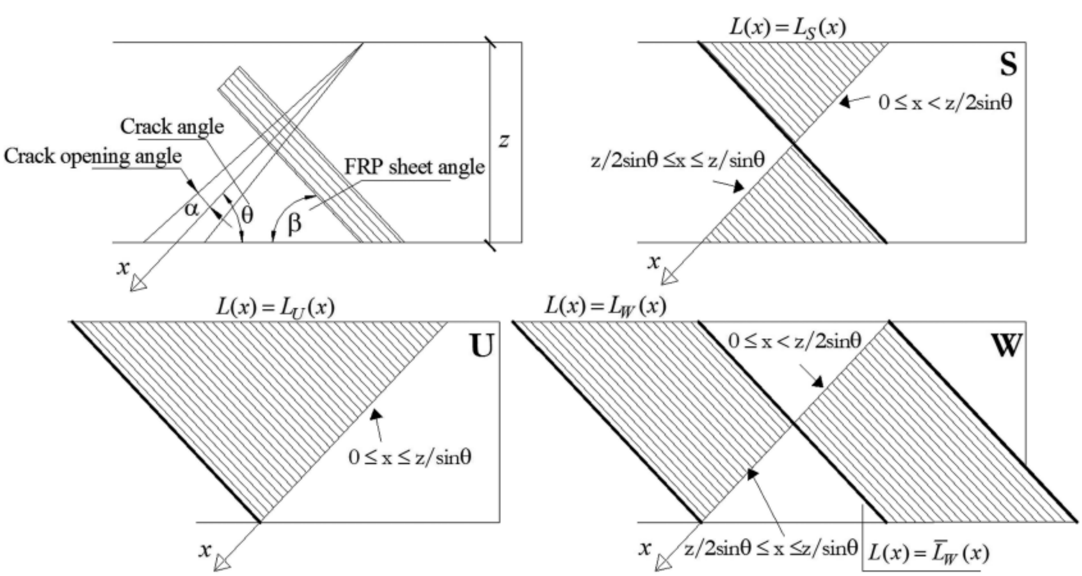

Figure 8.
Boundary conditions (available bond length) for three strengthening configurations: S = Side bonding, U = U-jacketing, and W = Wrapping

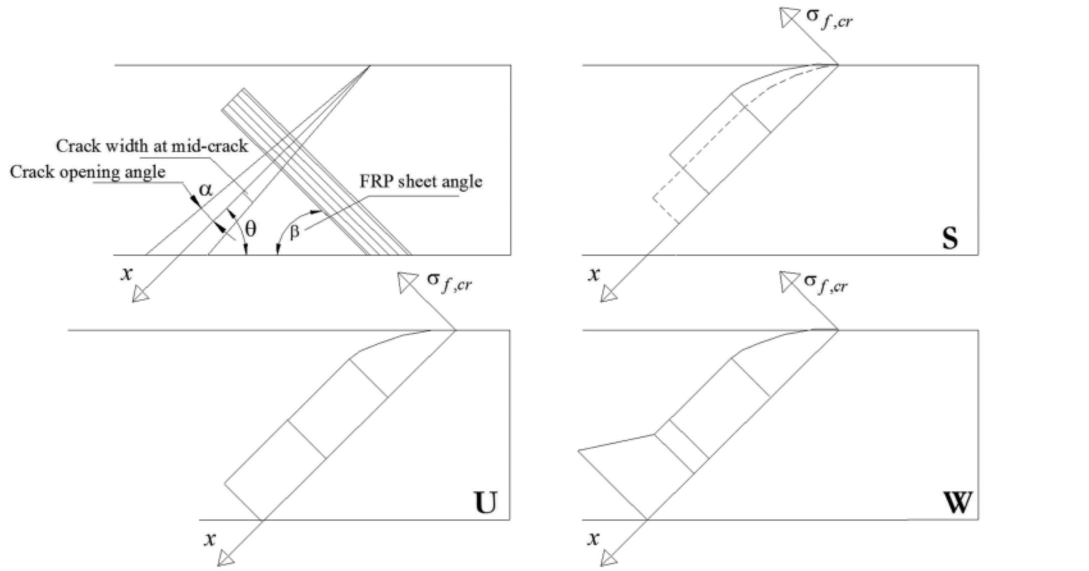

Figure 9.
Typical stress profiles in FRP sheets along the shear crack for three strengthening patterns: S = Side bonding, U = U-jacketing, and W = Wrapping

Figure 9 qualitatively depicts the $\delta_{f,cr}(x)$ profiles along the crack for three different strengthening patterns considered, when sheets are used.

In pattern S, the stress profile is truncated near the end of the crack, where the available length tends to zero. In U, the stress profile remains constant, where the available length allows for full debonding strength to develop throughout the crack length. In W, the stress profile rises towards the end of the crack, where, after complete debonding, the sheet is restrained at both ends and subjected to pure tension, up to its tensile strength. Also in this case, a closed-form equations of $\delta_{f,cr}(x)$ can be found in [15].

3.6. Determination of FRP contribution to the shear capacity

The objective is to obtain the maximum contribution of the FRP strips/sheet to the shear capacity. This means to identify, among all possible shapes of the FRP stress profile $\delta_{f,cr}$ $[u(\alpha,x), l_b(x)]$, which changes with the crack opening α, the one offering the maximum contribution, for each strengthening pattern.

3.6.1. Effective stress in the FRP sheet

For this purpose it is expedient to define an *effective stress* in the FRP sheet as mean FRP stress field $\delta_{f,cr}(x)$ along the shear crack length $z/\sin\theta$:

$$\sigma_{fe}(\alpha) = 1/(z/\sin\theta)\cdot\int_0^{z/\sin\theta}\sigma_{f,cr}[u(\alpha,x),l_b(x)]\,dx \qquad (14)$$

which might be regarded as an equivalent constant FRP stress block along the shear crack, inclined at the same angle   of the FRP fibres, as the crack gradually opens.

The integral (14) has closed-form solutions, that can be found again in [15].

3.6.2. Effective debonding strength

The maximum FRP effective stress, termed the *effective debonding strength* f_{fed}, is found by imposing:

$$d\sigma_{fe}(\alpha)/d\alpha = 0 \qquad (15)$$

Solution of (15) allows to determine the FRP stress profile with the maximum area, i.e., the effective debonding strength of the FRP shear strengthening.

In case of S-strengthening (neglecting the analytical developments presented in [15]) one has:

$$f_{fed} = f_{fdd}\cdot z_{rid,eq}/\min\{0.9d,h_w\}\cdot\left(1-0.6\sqrt{l_{eq}/z_{rid\ eq}}\right)^2 \qquad (16)$$

where :

$$z_{rid,eq} = \min\{0.9d,h_w\}-\left(l_e-s_f/\left(f_{fdd}/E_f\right)\right)\cdot\sin\beta \qquad (17)$$

Note that $z_{rid,eq}$ is equal to the vertical projected length of the FRP strip, minus the effective bond length where bond is building up, plus a bonded length that would be necessary if the FRP stress was uniform under the debonding slip s_f.

In case of U-strengthening:

$$f_{fed} = f_{fdd} \cdot \left[1 - \left(l_e \sin\beta / \min\{0.9d, h_w\}\right)/3\right] \quad (18)$$

In case of W-strengthening:

$$f_{fed} = f_{fdd} \cdot \left[1 - \left(l_e \sin\beta / \min\{0.9d, h_w\}\right)/6\right] + \quad (19)$$
$$+\left(\phi_R \cdot f_{fd} - f_{fdd}\right)/2 \cdot \left[1 - \left(l_e \sin\beta / \min\{0.9d, h_w\}\right)\right]$$

where f_{fd} is the design ultimate strength of the FRP.

3.7. Shear capacity with FRP

In case when the reinforcement type is U or W, the Mörsch resisting mechanism can be activated and the shear carried by FRP is expressed as:

$$V_{Rd,f} = 0.9d/\gamma_{Rd} \cdot f_{fed} \cdot 2t_f \cdot (\cot\theta + \cot\beta) \cdot w_f / p_f \quad (20)$$

while for side-bonding (S) the FRP role is "bridging" the shear crack, so that:

$$V_{Rd,f} = \min\{0.9d, h_w\}/\gamma_{Rd} \cdot f_{fed} \cdot 2t_f \cdot \sin\beta/\sin\theta \cdot w_f / p_f \quad (21)$$

with d = beam effective depth,

f_{fd} = design effective strength of the FRP shear strengthening, given by (16) for S, by (18) for U and by (19) for W

t_f = thickness of FRP strip/sheet (on single side) with angle β

s_f, w_f are strip spacing and width, respectively, measured orthogonally to direction β.

Assuming cracks inclined at θ = 45° with respect to the vertical and strips/sheets vertically aligned at β = 90°, the two previous equations become:

$$V_{Rd,f} = 0.9d/\gamma_{Rd} \cdot f_{fed} \cdot 2t_f \cdot w_f / p_f \quad (22)$$

$$V_{Rd,f} = \min\{0.9d, h_w\}/\gamma_{Rd} \cdot f_{fed} \cdot 2t_f \cdot \sqrt{2}\, w_f / p_f \quad (23)$$

The design shear capacity is given by:

$$V_{Rd} = \min\{V_{Rd,ct} + V_{Rd,s} + V_{Rd,f}, V_{Rd,\max}\} \quad (24)$$

where $V_{Rd,ct}$ is the concrete contribution, given by (e.g., [16]):

$$V_{Rd,ct} = 0.18/\gamma_c\, b_w \cdot d \cdot \min\left\{1 + \sqrt{200\ mm/d}, 2\right\} \cdot \sqrt[3]{100 \cdot \min\{0.02, \rho_{sl}\} \cdot f_{ck}} \quad (25)$$

(γ_c = concrete partial safety factor, b_w = web section width) and $V_{Rd,s}$ is the steel contribution, given by:

$$V_{Rd,s} = 0.9d \cdot f_{yd}\, n_{st} \cdot A_{st}/s_{st}\, (\cot\theta + \cot\beta_{st}) \sin\beta_{st} \quad (26)$$

(ρ_{sl} = longitudinal reinforcement ratio, f_{ck} = concrete characteristic cylindrical strength, f_{yd} = design steel yield strength, n_{st} = transverse reinforcement legs number, A_{st}, s_{st} = area (one leg) and spacing of stirrups, and β_{st} = stirrups angle)

In (24), $V_{Rd,max}$ is the concrete strut strength, given by (e.g., [16]):

$$V_{Rd,\max} = 0.9d \cdot b_w \cdot \nu \cdot f_{cd} \cdot (\cot\theta + \cot\beta_{st}) / (1 + \cot^2\theta) \quad (27)$$

with $\nu = 0.6[1 - f_{ck}/250]$ [in MPa]. (28)

4. VALIDATION OF DESIGN EQUATIONS

The above equations are validated by their fitting to the experimental results from the tests presented above as well as from tests in literature ([17], [18], [19], [20], [21], [22], [23], [24], [3], [25], [26], [7], [28]), for a total of 60 tests. A complete detailed list of tests by other authors, used to validate the above equations, can be found in [28].

The results are presented in Figure 10, where trend lines are shown, too. Mean values of the material properties were used and partial factors were set to 1, for comparisons with experimental results. In tests with variable slope of the FRP strips, an average value of 45° was considered, while the spacing is horizontal. The shear capacity of the reference beam was computed as the mean between the four tested unstrengthened specimens. Note that in specimen SS90, SS45, and US90, contribution of FRP strengthening was not considered, as it was observed that the diagonal shear cracks did not cross the strips.

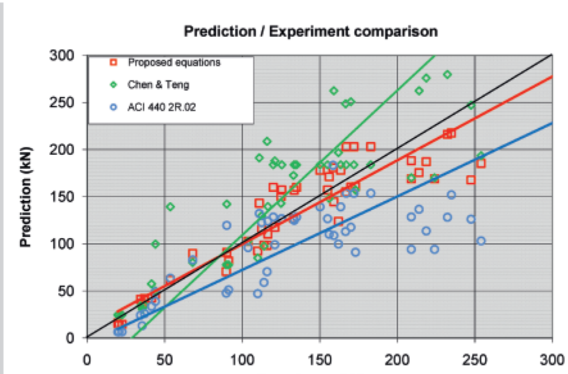

Figure 10.
Prediction/experiment comparison with: the proposed equations, Chen and Teng (2003) model, and ACI (2002) equations

The mean error, in predicting shear capacity of the beams where FRP was activated, is 7%, with a peak of 15% for patterns US60 and UF90, which is acceptable. Looking at the trend lines, the proposed equations predict experimental results with quite satisfactory accuracy.

The predictions obtained with the proposed equations are also compared with those obtained with a different model [5], for the FRP contribution, and with the equations adopted in [27], for both concrete and FRP contributions.

5. CONCLUSIONS

A fundamental problem in the analytical definition of the shear capacity of reinforced concrete beams, strengthened with externally bonded Fibre Reinforced Polymers (FRP) was examined, and a possible solution –a mechanics-based– model for the shear capacity has been proposed, as opposed to existing regression-based models.

The model was obtained through the following steps, with due consideration of underlying physical mechanisms:

- a) the generalised constitutive law of an FRP layer bonded to concrete is defined;
- b) the compatibility imposed by the shear crack opening and the appropriate boundary conditions – which depend on the strengthening pattern (side bonding, U-jacketing or wrapping) – are included in the formulation;
- c) equations of the stress field in the FRP strip/sheet crossing a shear crack are obtained.

Closed-form equations were defined for the effective debonding strength, as function of both adopted strengthening pattern and some basic geometric and mechanical parameters.

In particular, regarding so-called "effective" debonding strength of FRP strips/sheets crossing shear cracks, closed-form equations were found, for computing the FRP contribution V_f to the overall shear capacity. In this respect, it has been clarified that V_f should be computed, for U- and W-strengthening patterns, considering a Mörsch truss mechanism, whereas, for S-strengthening, considering a "crack-bridging" mechanism.

The equations accuracy has been verified versus the experimental shear strength of R/C beams, collected from tests in literature and from the research purposely carried out on under-designed real-scale beams, strengthened with different FRP patterns. They showed good correlation with all and no *a posteriori* calibration of the model was performed.

The effectiveness of the equations has been finally compared to other approaches available in the literature.

The proposed equations have been included in the Italian FRP-strengthening design Code [10].

ACKNOWLEDGEMENTS

The authors wish to thank the Interbau srl company, Milan, Italy, for casting the beam specimens and applying the CFRP strengthening.

REFERENCES

[1] *Monti G., Santinelli F., Liotta M.A.*; Shear strengthening of beams with composite materials. Proc. 2nd International Conference on FRP Composites in Civil Engineering CICE 2004, Adelaide, Australia, December 2004

[2] *Täljsten B.*; Strengthening of concrete structures for shear with bonded CFRP-fabrics. Recent advances in bridge engineering, Advanced rehabilitation, durable materials, nondestructive evaluation and management, Eds. U. Meier and R. Betti, Dübendorf, 1997, p.57-64

[3] *Triantafillou, T. C.*; Shear strengthening of reinforced concrete beams using epoxy-bonded FRP composites. ACI Structural Journal, 95(2), March-April, 1998; p.107-115

[4] *Khalifa A., Gold W.J., Nanni A., Aziz A.M.I.*; Contribution of externally bonded FRP to shear capacity of RC flexural members. ASCE Journal of Composites for Construction, 2(4), 1998; p.195-202

[5] *Chen J.F., Teng J.G.*; Shear capacity of FRP strengthened RC beams: FRP debonding., ASCE, Journal of Structural Engineering, Vol. 129, 2003; p.615-625

[6] *Adhikary B.B., Mutsuyoshi H.*; Behavior of Concrete Beams Strengthened in Shear with Carbon-Fiber Sheets. ASCE, Journal of Composites for Construction, Vol. 8, 2004; p.258-264

[7] *Deniaud C., Cheng J.J.R.*; Simplified shear design method for concrete beams strengthened with FRP. ASCE, Journal of Composites for Construction, Vol.8 (5), 2004; p.425-433

[8] *Triantafillou T. C., Antonopoulos C. P.*; Design of concrete flexural members strengthened in shear with FRP. ASCE Journal of Composites for Construction, Vol. 4 (4), 2000; p.198-205

[9] *fib*; Design and Use of Externally Bonded FRP Reinforcement (FRP EBR) for Reinforced Concrete Structures. Bulletin no. 14, fib Task Group 9.3 "FRP Reinforcement for Concrete Structures", 2001

[10] *CNR*; Instructions for design, execution and control of strengthening interventions through fiber-reinforced composites. CNR-DT 200/04, Consiglio Nazionale delle Ricerche, Rome, Italy (English version), 2005

[11] *Menegotto M., Monti G.*; Strengthening Concrete and Masonry with FRP – A New Code of Practice in Italy. 5th AMCM Conference, Gliwice-Ustroń, Poland, June 2005

[12] *Chen J. F., Teng J.G.*; Anchorage strength models for FRP and steel plates bonded to concrete. ASCE, Journal of Structural Engineering, Vol.127, 2001; p.784-791

[13] *Monti G., Renzelli M., Luciani P.*; FRP Adhesion to Uncracked and Cracked Concrete Zones. 6th International Symposium on Fibre-Reinforced Polymer (FRP) Reinforcement for Concrete Structures (FRPRCS-6), Singapore, 2003

[14] *Campione G., Miraglia N.*; Strength and strain capacities of concrete compression members reinforced with FRP. Cement and Concrete Composites, Elsevier, 25, 2003; p.31-41

[15] *Monti G., Santinelli F., Liotta M.A.*; Mechanics of FRP shear strengthening of RC beams. Proc. ECCM 11, Rhodes, Greece, May 2004

[16] *CEN*; Eurocode 2: Design of concrete structures – Part 1-1: General rules and rules for buildings. prEN 1992-1-1:2003 E, Comité Européen de Normalisation, Brussels, Belgium, 2003

[17] *Al-Sulaimani G.J., Sharif A., Basunbul I.A., Baluch M.H., Ghaleb B.N.*; Shear Repair for Reinforced Concrete by Fiberglass Plate Bonding. ACI Structural Journal, Vol.91 (3), 1994; p.458-464

[18] *Chajes M.J., Januszka T.F., Mertz D.R., Thomson T.A. Jr., Finch W.W. Jr.*; Shear Strengthening of Reinforced Concrete Beams Using Externally Applied Composite Fabrics, ACI Structural Journal, Vol. 92 (3), 1995; p.295-303

[19] *Funakawa I., Shimono K., Watanabe T., Asada S.*, Ushijima S.; Experimental study on shear strengthening with continuous fiber reinforcement sheet and methyl methacrylate resin, III Int. Symp. Non Metallic (FRP) Reinforcement for Concrete Structures, Japan, 1997; p.475-482

[20] *Kamiharako A., Maruyama K., Takada K., Shimomura T.*; Evaluation of shear contribution of FRP sheets attached to concrete beams, III Int. Symp. Non Metallic (FRP) Reinforcement for Concrete Structures, Japan, 1997; p.467-474

[21] *Norris T., Saadatmanesh H., Ehsani M.R.*; Shear and Flexural Strengthening of R/C Beams with Carbon Fiber Sheets, ASCE, Journal of Structural Engineering, Vol. 123 (7), 1997; p.903-911

[22] *Taerwe L., Khalil H., Matthys S.*; Behaviour of R/C beams strengthened in shear by external CFRP sheets, III Int. Symp. Non Metallic (FRP) Reinforcement for Concrete Structures, Japan, 1997; p.483-490

[23] *Umezu K., Fujita M., Nakai H., Tamaki K.*; Shear behavior of RC beams with aramid fiber sheet, III Int. Symp. Non Metallic (FRP) Reinforcement for Concrete Structures, Japan, 1997; p.491-498

[24] *Challal O., Nollet M.J., Saleh K.*; Use of CFRP Strips for Flexure and Shear Strengthening of RC Members. 2nd Int. Conference on Composites in Infrastructure, Tucson, AZ, USA, 1998; p.249-260

[25] *Khalifa A., Nanni A.*; Improving shear capacity of existing RC T-section beams using CFRP composites. Cement & Concr. Comp., Vol. 22, 2000; p.165-174

[26] *Park S.Y., Naaman A. E., Lopez M.M., Till R.D.*; Shear strengthening effect of R/C beams using glued CFRP sheets, Int. Conf. On FRP Composites in Civil Engineering, Hong Kong, China, 1, 2001; p.669-676

[27] *ACI*; ACI440.2R-02 – Guide for the Design and Construction of Externally Bonded FRP Systems for Strengthening Concrete Structures. American Concrete Institute, Committee 440; 2002

[28] *Aprile A., Benedetti A.*; Coupled flexural-shear design of RC beams strengthened with FRP. Composites Part B: Engineering. Volume: 35, Issue: 1, January, 2004; p.1-25

[29] *Brosens K., Van Gemert D.*; Anchorage design for externally bonded carbon fiber reinforced polymer laminates. Proc. 4th Int. Symposium on FRP Reinforcement for Concrete Structures, Baltimore, USA, 1999; p.635-645

[30] *Monti G., Liotta M.A.*; Tests and design equations for FRP-strengthening in shear. Journal of Construction and Building Materials. Volume 21, Issue 4, April, 2007; p.799-809